Mapping the Electron Transfer Interface between Cytochrome b_5 and Cytochrome c[†]

Yi Ren,[‡,§] Wen-Hu Wang,[‡] Yun-Hua Wang,[‡] Martin Case,[§] Wen Qian,[‡] George McLendon,*[,§] and Zhong-Xian Huang*[,‡]

Chemical Biology Laboratory, Department of Chemistry, Fudan University, Shanghai 200433, China, and Department of Chemistry, Princeton University, Princeton, New Jersey 08544

Received November 20, 2003; Revised Manuscript Received February 3, 2004

ABSTRACT: To characterize the cytochrome b_5 (Cyt b_5)−cytochrome c (Cyt c) interactions during electron transfer, variants of Cyt b_5 have been employed to assess the contributions of electrostatic interactions (substitution of surface charged residues Glu44, Glu48, Glu56, and Asp60 and heme propionate), hydrophobic interactions, and the thermodynamic driving forces (substitutions for hydrophobic residues in heme pocket residues Phe35, Pro40, Val45, Phe58, and Val61). The electrostatic interactions play an important role in maintaining the stability and specificity of the Cyt b_5−Cyt c complex that is formed. There is no essential effect on the intraprotein complex electron transfer even if most of the involved negatively charged residues on the surface of Cyt b_5 have been removed. The results support a dynamic docking paradigm for Cyt b_5−Cyt c interactions. The orientation that is optimal for binding may not be optimal form for electron transfer. Substitution of hydrophobic residues does not have a significant effect on the binding between Cyt b_5 and Cyt c; rather, it regulates the electron transfer rates via changes in the driving force. Combining the electron transfer studies of the Cyt b_5−Cyt c system and the Cyt b_5−Zn−Cyt c system, we obtain the reorganization energy (0.6 eV) at an ionic strength of 150 mM.

Electron transfer (ET) reactions of metalloproteins play essential roles in important biological processes such as photosynthesis and respiration (*1*). Many studies have been directed toward the elucidation of the mechanisms of interaction between ET partners. One of the most widely studied systems is the complex between cytochrome b_5 (Cyt b_5) and cytochrome c (Cyt c). This ET system has been under intensive experimental and theoretical investigation over a period of nearly 30 years (*2*−*5*). Recent studies (*6*) suggest that Cyt b_5−Cyt c interactions may be employed in intracellular signaling, regulation of cytochrome P450-dependent reactive oxygen species (ROS) production, and apoptosis.

Specific molecular recognition contributes to the physiological specificity in transferring an electron; in previous studies, electrostatic interactions have been recognized as a crucial factor for Cyt b_5−Cyt c complexation. The first detailed computer simulation structural model of the 1:1 Cyt b_5−Cyt c complex was proposed by Salemme (*7*). The complex is assumed to be stabilized by electrostatic interactions: Glu44−Lys27, Glu48−Arg13, Asp60−Lys72, and heme propionate−Lys79 (first and second components from Cyt b_5 and Cyt c, respectively). From the Brownian dynamics simulation, Northrup (*8*) proposed another docking model, which also involves a quartet electrostatic interaction: Glu48−Arg13, Glu56−Lys87, Asp60−Lys86, and heme propionate−Tml72. When these two protein complexes were subjected to energy minimization, the final protein complexes are significantly different from those originally proposed. The simulations by Guillemette (*9*) indicated that electrostatic interactions at the molecular interface result in a flexible association complex. Indeed, our previous studies indicated that certain binding geometries other than Salemme and Northrup models do occur (*10*−*12*). With regard to the ET process, the exact pathway by which an electron travels from Cyt b_5 to Cyt c is still unknown. Recent studies (*13, 14*) on the ET system of the Cyt b_5−Mb complex showed that the orientation optimal for binding might not be optimal for electron transfer. Their results support a "dynamic docking" paradigm for protein−protein interactions in which numerous weakly bound conformations of the docked complex contribute to the binding of Cyt b_5 to Mb; however, only a very small subset of these are ET active, and this subset does not include the conformations most favorable for binding. Might a similar mechanism be at work in the Cyt b_5−Cyt c system? Obviously, we need more thorough studies on the dynamic interactions and ET process between Cyt b_5 and Cyt c.

This report extends previous studies by assessing the contributions of amino acid residues in Cyt b_5 that are expected to influence the docking and ET between Cyt b_5 and Cyt c. The factors that are addressed in this study include the role of electrostatic interactions (substitutions of surface charged residues Glu44, Glu48, Glu56, and Asp60 and heme propionate), hydrophobic interactions, and the thermodynamic driving force (substitution of hydrophobic residues in heme pocket residues Phe35, Pro40, Val45, Phe58, and Val61). Previous X-ray and NMR studies (*10*−*12, 15*−*17*) indicated that mutations do not result in significant alterations in the protein's overall structure. In this paper, we report a combined study of interprotein and intraprotein complex ET by stopped-flow methods (Cyt b_5−Cyt c) and laser-flash

[†] This project was supported by the National Science Foundation of China.

* To whom correspondence should be addressed. Z.-X.H.: telephone, +86-21-65643973; fax, +86-21-65641740; e-mail, zxhuang@fudan.edu.cn. G.M.: telephone, (609) 258-6808; e-mail, GLM@princeton.edu.

[‡] Fudan University.

[§] Princeton University.

10.1021/bi036078k CCC: $27.50
Published on Web 03/05/2004

photolysis (Cyt b_5−Zn−Cyt *c*), as well as Brownian dynamics simulation of some variants of the Cyt b_5−Cyt *c* system.

MATERIALS AND METHODS

General Methods. Water purified with a Vaponics Pure System to a resistance of 17−18 MΩ was used in the preparation of all solutions. The pH was measured using a Metrohm 654 pH meter equipped with a Russell combined pH electrode. Proflavine hemisulfate and methylviologen were purchased from Tokyo Chemical Industry Co. Ltd. Cyt *c* (horse heart) was purchased from Sigma. All other chemicals were analytical grade.

Protein Preparations. Trypsin-solubilized bovine liver microsomal Cyt b_5 variants [wild-type (WT) Cyt b_5 and the E44A, E56A, E44/56A, E44/48A, E48/56A, E48A/D60A, E44/48/56A, E44/56A/D60A, E48/56A/D60A, E44/48/56A/D60A, F35Y, F35L, P40V, V45H, V45E, F58Y, F58W, V61H, and V61E mutants] were constructed and expressed in *Escherichia coli* as previously described (*12*, *15*, *18*−*24*). Dimethyl ester heme-substituted derivatives of Cyt b_5 (wild-type Cyt b_5−DME and E44/48/56A/D60A−DME) were prepared from WT Cyt b_5 and its E44/48/56A/D60A mutant by the method of Reid (*25*). Zinc-substituted Cyt *c* (ZnCc) was prepared as previously described (*26*−*28*).

UV−*Visible Difference Spectra.* Binding constants of the Cyt b_5−Cyt *c* complex were measured by the previously established method (*10*). Protein solutions were prepared by dissolving the proteins in sodium phosphate buffer ($I = 1$ mM, pH 7.0). Difference spectra were determined using a tandem mixing cell with a path length of 2 × 0.438 cm on an HP8453 diode array spectrophotometer at 25 °C. In the titration experiments, the Cyt b_5 concentration was held constant (6.0 μM) and the Cyt *c* concentration varied from 2 to 20 μM.

Stopped-Flow Measurements. Rapid-mixing experiments were performed with an AF-61DX2 double-mixing stopped-flow spectrophotometer (observation path length of 2 mm). The temperature was maintained with a NESLAB RTE-5B circulating bath instrument with a precision of ±0.2 °C. The conditions were the same as in previous studies (*15*). All protein solutions contained 10 mM EDTA, sodium phosphate ($I = 50$ mM, pH 7.0), and KCl, which was used to adjust the ionic strength. The solutions containing Cyt b_5 and ferricytochrome *c* were placed in Schlenk tubes that were sealed with cleaned serum stoppers. Solutions were thoroughly deoxygenated by bubbling prepurified nitrogen for 30 min, which had been passed through a hot Cu_2O tower and two methylviologen and one photoreduced proflavin scrubbing tower. After 30 min, 1/1000 (v/v) of the methylviologen/proflavin mixture (each at 1 mM) was introduced into the Cyt b_5 solution with a gastight syringe, and Cyt b_5 was photoreduced with a 100 W incandescent lamp situated 15 cm from the reaction tube for 30 min. Then, the solutions were transferred into the two reservoir syringes of the apparatus, which had been filled with purified nitrogen. The reactions were performed under pseudo-first-order conditions. Oxidation of ferrocytochrome b_5 was monitored at 428 nm where the total absorbance and the change in the absorbance of Cyt *c* are small. At least 10 absorbance traces were averaged and fitted to a first-order rate expression to generate the ET rate (appended on KinetAsyst).

Laser-Flash Photolysis Measurements. Flash photolysis was carried out as previously described (*29*). We use a Quanta Ray GCR-170 Nd:YAG laser/MOPO-710 (Spectra Physics) with a 7 ns pulse width. The excitation wavelength was 532 nm. The ET kinetics were monitored by recording absorbance difference spectra as a function of time. Difference spectra were collected using an 1103 EG&G Xe flash lamp probe source and a Princeton Instruments IRY-700/15 image intensifier diode array detector. The image intensifier was gated for 20 ns using an Avtech AVRL-1-PS pulse generator. Timing synchronization of the intensifier, flash lamp probe, and diode array detector readout was controlled using a Stanford Research Systems DG535 delay gate generator. This methodology is the same as that of Goldbeck and Kliger (*30*), except that timing synchronization was taken from the laser Q switch. Concentrated protein solutions, sodium phosphate buffer ($I = 1$ mM, pH 7.0), and sodium chloride solutions (4 M) were degassed and transferred to a glovebox. Proteins were mixed and diluted to a certain concentration and ionic strength in the glovebox. Difference spectra were recorded from 50 ns to 50−500 ms after laser photolysis. Approximately 35 points were recorded for each sample; each was averaged over four shots. Data were analyzed using Matlab (Mathworks Inc.). Kinetic rates were calculated with singular-value decomposition of time−wavelength−intensity matrices as described by Hofrichter *et al.* (*31*).

Brownian Dynamic Simulations. Brownian dynamic (BD) simulations were performed with the Macrodox program developed by Northrup and co-workers at Tennessee Technological University (Cookeville, TN). The details of BD simulations of protein−protein interaction have been described elsewhere (*32*, *33*). Briefly, the coordinates of Cyt *c* (Protein Data Bank entry 1CYO), ZnCc (1M60), Cyt b_5 (1EHB), Cyt b_5 E44/48/56A/D60A (1F03), WT Cyt b_5−DME (1MNY), Cyt b_5 F35Y (1M20), Cyt b_5 V45E (1LQX), and Cyt b_5 V61H (1ES1) were downloaded from the Protein Data Bank. In the program, charges are assigned on the basis of the pK_a values estimated by the Tanford−Kirkwood calculation. On the basis of those assigned charges, a Poisson−Boltzmann calculation is performed to determine the electrostatic potential grid surrounding Cyt b_5. In the simulation, Cyt *c* is simply treated as an array of test charges in the field of Cyt b_5 without considering its internal low dielectric. The simulation starts with the center of Cyt *c*, 65 Å from the Cyt b_5 potential grid. The Brownian motion of Cyt *c* in the field of Cyt b_5 was simulated stochastically by a series of small displacements governed by the Smoluchowski diffusion equation with forces. A trajectory would be declared to be successful if the distance between any meso carbon (C_M) of one heme reaches a prescribed distance from any C_M of the partner heme at any time before Cyt *c* passes outside an escape radius of 200 Å. For each successful trajectory, the position of Cyt *c* at the instant of contact with the surface of Cyt b_5 is recorded, although the trajectories were not truncated until the outer 200 Å sphere was reached. For each simulation, at least 10 000 trajectories were calculated at pH 7.0 and an ionic strength of 150 mM on the Red Hat Linux system of the computer. A simulation generated a large set of complexes; they are represented here as a so-called docking profile, in which the centers of mass of Cyt *c* in each complex are represented as dots surrounding Cyt b_5.

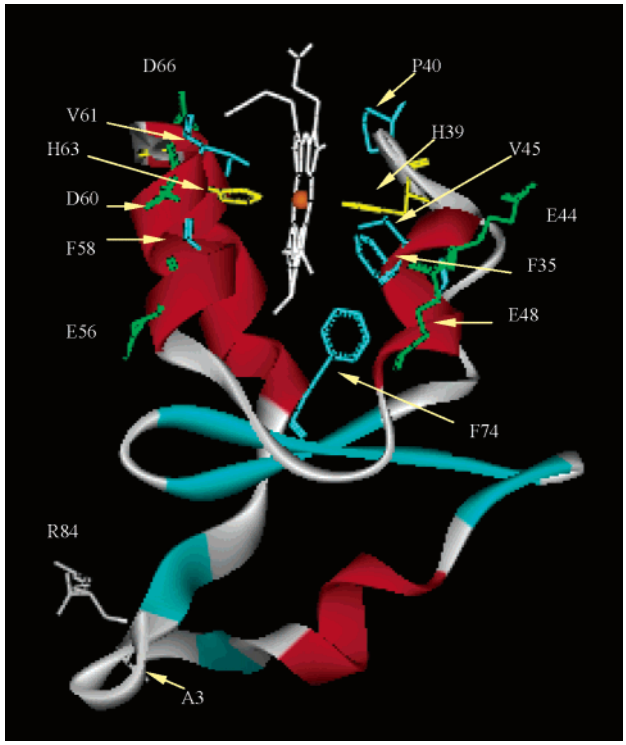

FIGURE 1: Ribbon diagram of wild-type Cyt Tb_5. The side chains of Phe35, Pro40, Val45, Phe58, and Val61 are shown in cyan and those of Glu44, Glu48, Glu56, Asp60, and Glu66 in green. His39 and His63 are shown in yellow. Ala3 and Arg84 are denoted. This diagram was prepared using ViewerLite.

RESULTS

Mutational Design Strategy

The trypsin-solubilized fragment of Cyt b_5 contains 84 amino acid residues. Heme is bound in a hydrophobic pocket with the wall and the bottom composed of four α-helices and three β-strands, respectively (shown in Figure 1). Glu44, Glu48, Glu56, Asp60, and heme propionate are negatively charged groups located at the molecular surface and are considered to be involved in the interprotein interactions with Cyt c. To better investigate the electrostatic interactions on the Cyt b_5−Cyt c docking, we generated the following Cyt b_5 variants: E44A, E56A, E44/56A, E44/48A, E48/56A, E48A/D60A, E44/48/56A, E44/56A/D60A, E48/56A/D60A, E44/48/56A/D60A mutants, Cyt b_5−DME, and E44/48/56A/D60A−DME. Val45 and Val61 are component residues of the heme pocket wall and form van der Waals interactions with the heme. Both Val45 and Val61 are located at the edge of the heme pocket but at the opposite sides of the heme plane. Previous studies indicated that the hydrophobic contacts involving Val28, Ala81, and Phe82 of Cyt c and Val45 and Val61 of Cyt b_5 are present in the complexes generated via theoretical simulation. We employ the V45E, V45H, V61E, and V61H mutants of Cyt b_5 to evaluate the contributions of hydrophobic interactions. Phe35 and Pro40 are two of the component residues of a hydrophobic patch on the Cyt b_5 surface. Residues Phe35 and Phe/Tyr74 also form an aromatic channel with His39, one of the axial heme b ligands. The F35Y, F35L, and P40V mutants of Cyt b_5 were studied to gain further insight into the roles of the hydrophobic patch and/or aromatic channel, which might be important in the ET process. Furthermore, Phe35 as well as Phe58 also stabilizes heme binding through hydrophobic aromatic stacking with the heme ring. The F58Y and F58W mutants of Cyt b_5 were studied. The mutations do not generally change the UV−visible spectra of Cyt b_5, indicating mutations do not result in significant alterations in the protein's overall structures, which are proven by determination of crystal and solution structures of most of the Cyt b_5 variants; however, the latter analyses demonstrate that the local conformational changes do occur.

Table 1: Comparison of the Effects of the Mutation on the Cyt b_5−Cyt c Interaction

protein	E_0' (mV)	K_A ($\times 10^6$ M^{-1})	k_{12} (stopped-flow) ($\times 10^6$ M^{-1} s^{-1}) (I = 150 mM)	k (photolysis) ($\times 10^5$ s^{-1}) (I = 1 mM)
WT Cyt b_5	5.0[c]	4.7 (0.022)[a]	96.6	5.5
E44A	6.0[b]	1.9[b]	48.0	4.6
E56A	7.5[b]	2.7[b]	65.3	9.3
E44/56A	7.5[b]	1.1[b]	46.6	7.5
E44/48A	10.0[c]	0.4	35.4	8.9
E48/56A	8.0[c]	0.3	47.6	11.0
E48A/D60A	7.0[c]	0.4[d]	46.7	9.6
E44/48/56A	12.0[c]	0.2	39.7	9.1
E44/56A/D60A	8.0[c]	−, (0.013)[a]	32.2	10.0
E48/56A/D60A	13.0[c]	0.1, (0.011)[a]	40.8	14.0
E44/48/56A/D60A	15.0[c]	−, (0.005)[a]	30.1	second order
Cyt b_5−DME	70.0[e]	1.0	11.8[f]	3.0
E44/48/56A/D60A−DME	77.0[e]	−	8.0[f]	second order

[a] Conditional binding constants measured by NMR (*10*). [b] From ref *15*. [c] From ref *18*. [d] From ref *19*. [e] Spectroelectrochemical measurements, in 100 mM phosphate buffer (pH 7.0). [f] I = 350 mM.

Table 2: Comparison of the Effects of the Mutation on the Cyt b_5−Cyt c Interaction

protein	E_0' (mV)	k_{12} ($\times 10^6$ M^{-1} s^{-1}) stopped-flow	k_{12} ($\times 10^6$ M^{-1} s^{-1}) photolysis	k(photolysis) ($\times 10^5$ s^{-1})
WT Cyt b_5	5	96.6	2.2×10^2	5.5
F35Y	−64[a]	82.5	1.4×10^2	5.2
F35L	−26[a]	68.8	1.5×10^2	5.1
V61H	26[a]	40.9	1.3×10^2	5.3
V61E	−10[a]	72.0	1.7×10^2	5.9
V45H	8[a]	59.2	1.1×10^2	5.9
V45E	−26[a]	74.4	1.3×10^2	5.4
F58Y	31[a]	61.1	1.6×10^2	6.2
F58W	−2[a]	52.0	1.6×10^2	5.9
P40V	−43[a]	53.4	1.5×10^2	6.1
Cyt b_5−DME	70		1.3×10^2	3.0
E44/48/56A/D60A	15	30.1	0.9×10^2	second order
E44/48/56A/D60A−DME	77		0.4×10^2	second order

[a] Results obtained from our previous reports (*20*, *22*−*24*, *35*).

As indicated in Tables 1 and 2, mutations at surface residues of Cyt b_5 almost do not change the midpoint redox potentials of the variants; however, mutations at the heme pocket residues change the midpoint redox potentials essentially.

Binding of Cyt b_5 and Cyt c

The difference spectra in the region of 300−600 nm, which result from the interaction of Cyt c with Cyt b_5 variants, were recorded. The formation of the protein complex is evidenced by the intensity difference at the Soret band of these proteins, which is a measure of the extent of formation

of the protein complex as indicated in the literature (*34*). Because the binding between Cyt b_5 and Cyt *c* is in the direction of heme edge to heme edge, the change in the absorbance upon complex formation (ΔA) is directly proportional to the complex concentration and should follow the equation

$$\Delta A = (\Delta A_\infty/2b)\{c + b + 1/K_A - [(c + b + 1/K_A)^2 - 4cb]^{1/2}\}$$

where *c* and *b* represent the total concentration of Cyt *c* and Cyt b_5, respectively, ΔA_∞ is the value of ΔA with excess Cyt *c*, and K_A is the equilibrium association constant of Cyt *c* and Cyt b_5 variants. The K_A values were obtained by a nonlinear fitting program (Regression). The results are listed in Table 1.

Overall, neutralization of these surface charged groups, including Glu44, Glu48, Glu56, Asp60, and heme propionate, weakens the electrostatic interactions between Cyt b_5 and Cyt *c*, which indicates that all these groups participate in the binding between these two proteins. Meanwhile, the more charged groups are neutralized, the weaker the binding ability of these two proteins. We did not observe the difference spectra of the E44/56A/D60A, E44/48/56A/D60A, and E44/48/56A/D60A−DME variants of Cyt b_5 under this condition. We also noticed that the contribution of each of these five charged groups is not the same.

Though difference spectra of some mutants cannot be observed by UV−visible methods, electrostatic protein complexes do occur according to our previous study by NMR (*10*). The conditional binding constants decrease by 4-fold from WT Cyt b_5 (2.2×10^4 M^{-1}) to Cyt b_5 E44/48/56A/D60A (5.5×10^3 M^{-1}). These groups play an important role in formation of the electrostatic complex between Cyt b_5 and Cyt *c*. However, the influence of neutralization of charged residues involved in the Salemme and Northrup model is not as large as we expected.

As for those hydrophobic residues on the Cyt b_5 surface, our previous studies indicated that mutation at Phe35, Pro40, Phe58, and Val61 does not weaken the binding between Cyt b_5 and Cyt *c*. Nevertheless, the binding constants of the Val45 variants are lower than that of Cyt b_5.

Interprotein ET Studies by Stopped-Flow Kinetics

The kinetics of the interprotein ET ($I = 150$ mM, pH 7.0) between ferro-Cyt b_5 and ferric Cyt *c* were examined under pseudo-first-order conditions. Results are shown in Tables 1 and 2.

The interprotein ET rates measured at high ionic strengths incorporate many factors, including the ability to form a productive complex, electron transfer within the productive complex, and dissociation of the protein complex among others. Neutralization of surface charged residues (i.e., E44, E48, E56, D60, and heme propionate) does not change the ET driving force very much (see Table 1), so the observed differences mostly reflect the binding process. As there is for the Cyt b_5−Cyt *c* binding constants, there is a roughly cumulative effect for charge neutralization. Some mutants, such as E48A/D60A and E48/56A/D60A, rank relatively higher in ET rates, compared with their binding constants with Cyt *c*. It is possible that this reflects differences in ET rates in the productive protein complex, as a consequence of the mutation. For those mutants of hydrophobic residues (F35, V45, and V61), there is a rough E_0' dependence, reflecting the dependence of the rate upon driving force.

Interprotein and Intraprotein Complex ET Studies by Laser-Flash Photolysis

Intraprotein Complex ET at an Ionic Strength of 1 mM. The triplet excited state of ^{3}ZnCc decays with a rate constant of 100 ± 10 s^{-1} at room temperature. Decay of the triplet state in the Cyt b_5−Cyt *c* system at an ionic strength of 1 mM could be fitted very well with two exponential functions as Qin has described (*36*).

$$F(t) = A_1 \exp(-k_1 t) + A_2 \exp(-k_2 t)$$

Where *A* and *k* are the amplitude and first-order rate constant, respectively. The rate constant for the fast component of the decay was independent of the ZnCc concentration and of ionic strength. The rate constant k_2 for the slow component decreased as the protein concentration was decreased and as the ionic strength was increased. The relative amplitude of the fast component, $A_1/(A_1 + A_2)$, increased as the protein concentration was increased and as the ionic strength was decreased. It is clear that A_1 represents the intraprotein complex ET and A_2 represents the interprotein ET between Cyt b_5 and ZnCc. We examined the intraprotein complex ET between Cyt b_5 variants and ZnCc; data are shown in Tables 1 and 2. The results are an average of three separate experiments. Of the total decay amplitude, the fraction occupied by the intraprotein complex ET process (data not shown) indicates a degree of complexation between ZnCc and Cyt b_5, which is consistent with the binding constants measured by UV−visible difference spectra.

Most charge neutralization mutants enhance the observed ET rate with a maximum 2-fold effect, from 5.5×10^5 s^{-1} (Cyt b_5−ZnCc) to 1.4×10^6 s^{-1} (Cyt b_5 E48/56A/D60A−ZnCc). The ET rate of the Cyt b_5−DME−ZnCc complex (3.0×10^5 s^{-1}) is approximately half of that of the Cyt b_5−ZnCc complex. For the E44/48/56A/D60A and E44/48/56A/D60A−DME mutants, only the slow phase rate can be detected, which is consistent with the weak binding ability we have observed in the difference spectra. With respect to the pseudo-first-order rate constants, the former is 10 times faster. Obviously, esterification of the heme propionate considerably affects the ET process.

Mutations at Phe35, Pro40, Val45, Phe58, and Val61 have little effect on the ET rate constants.

Ionic Strength Titration of Protein ET Rates. We examined the pseudo-first-order ET of Cyt b_5, Cyt b_5−DME, and the E44/48/56A/D60A and E44/48/56A/D60A−DME mutants, under different ionic strengths ($I = 1-150$ mM). The sensitivity of k_{12} to ionic strength varies substantially for different mutants (Figure 3). The ET rate for WT Cyt b_5 decreases greatly with increasing NaCl concentrations, dropping by 25-fold as the salt concentration is increased from 20 to 150 mM. By comparison, the ET rate of the E44/48/56A/D60A−DME mutant dropped by only 4-fold under the same condition, suggesting that the electrostatic interaction was substantially weakened. Although neutralization of Glu44, Glu48, Glu56, Asp60, and heme propionate does not totally abolish the electrostatic interactions, these are the key

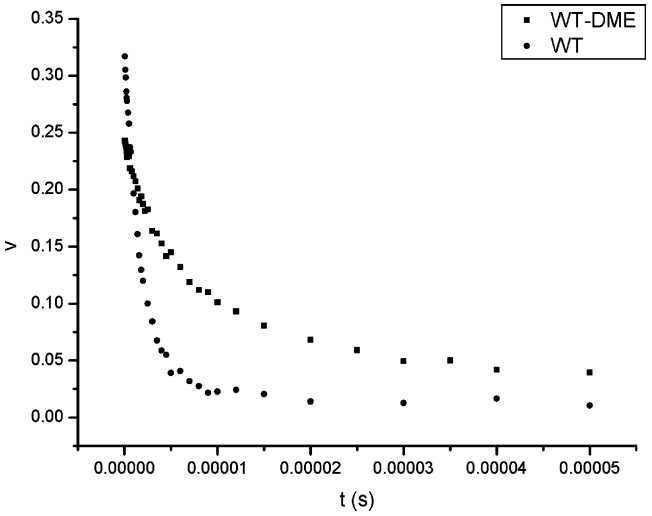

FIGURE 2: Kinetic traces of the dominant spectral profiles after SVD analysis.

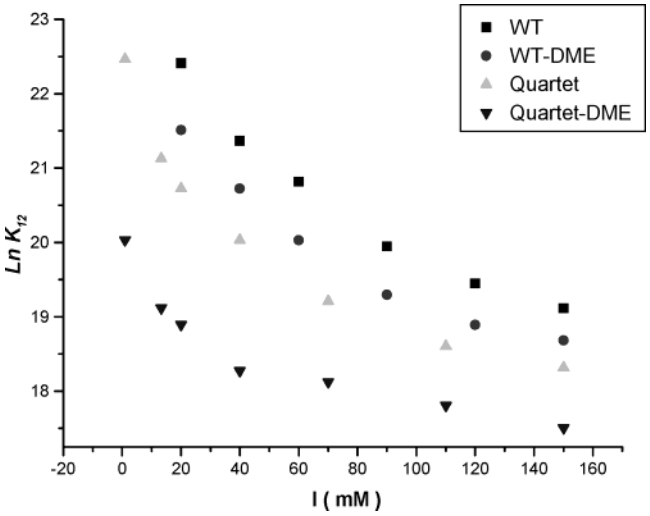

FIGURE 3: Pseudo-first-order ET rates between variants of Cyt b_5 and ZnCc at different ionic strengths by laser-flash photolysis.

groups that contribute to the electrostatic interactions between Cyt b_5 and Cyt c.

Interprotein ET at an Ionic Strength of 150 mM. We examined the reaction between WT Cyt b_5 and ZnCc, where the concentration of WT Cyt b_5 varied from 30 to 70 μM. The observed ET rates were proportional to the concentration of Cyt b_5. We also studied the ET between variants of Cyt b_5 and Cyt c under pseudo-first-order conditions with a Cyt b_5 concentration of 50 μM. As in the studies by the stopped-flow methods, the ET rates of Cyt b_5−DME and the E44/48/56A/D60A and E44/48/56A/D60A−DME mutants are slow, reflecting the difficulty in forming the precursor complex with Cyt c. For other mutants, there is no clear relation between ET rates and driving force. This is reasonable, since the driving force of Cyt b_5 and ZnCc is around 880 mV, which is much larger than the that of the reaction between Cyt b_5 and FeCyt c, and near the value of ΔG ($=\lambda$). Thus, the relatively small E_0' difference between variants of Cyt b_5 is not expected to significantly affect the observed rate.

Brownian Dynamics Simulation

Brownian dynamics (BD) simulations were employed to study the electrostatically controlled docking between variants of Cyt b_5 and Cyt c. With the pH set to 7.0 and the ionic strength set to 150 mM (the same condition as in our previous interprotein ET kinetics studies), a 100000-trajectory run with WT Cyt b_5 and the E44/48/56A/D60A mutant generated the docking profiles shown in Figure 4. In the docking profiles, WT and E44/48/56A/D60A Cyt b_5 are represented by the solid ribbon, and the mass centers of successfully docked Cyt c are represented with yellow dots. The criterion for productive docking is that the distance between meso carbons on the two porphyrin rings reach 16 Å. For the WT Cyt b_5−Cyt c system, 525 docked complexes were generated from 100 000 trajectories, compared with 1859 complexes generated for the Cyt b_5 E44/48/56A/D60A−Cyt c system. The distribution of "hits" is altered.

For the Cyt b_5−Cyt c system, the Cyt c dots are mainly populated around the heme-exposed edge side. In contrast, for the Cyt b_5 E44/48/56A/D60A−Cyt c system, the hits scatter almost uniformly around the whole hemisphere, incorporating the heme edge. We estimated the average monitor distances of all the successful trajectories. For the Cyt b_5 E44/48/56A/D60A−Cyt c system, the average distance between two heme irons is ~0.5 Å less than that in the WT Cyt b_5−Cyt c system within the encounter complexes found by the Brownian dynamics simulations. In our bovine liver microsomal Cyt *Tb*$_5$−horse heart Cyt c system, the surface charged groups on the surface of Cyt b_5 that contribute most are heme propionate, Glu44, Glu48, Glu56, and Asp60, a group similar to that with the Cyt *Lb*$_5$−yeast Cyt c system studied by Northrup *et al*. The contact-frequency histograms show the frequency with which the individual charged surface residues of variants of Cyt b_5 are involved in close ionic contacts; species−specific differences in the electrostatic docking of the Cyt b_5−Cyt c system are limited. With respect to the Cyt b_5−ZnCc system, the overall contribution of surface charged groups is similar with that of the Cyt b_5−Cyt c system. We noticed that the relative contribution of heme propionate is larger than that of the Cyt b_5−Cyt c system. Meanwhile, instead of Glu56, Asp66 plays a more important role. A high-pressure laser-flash photolysis study by the Morishima group (*37*) suggested that the docking of ZnCc with Cyt b_5 might be different from that with Cyt c. Zinc substitution could lead to perturbation on the electrostatic potential of the Cyt c protein surface and result in a different interaction with Cyt b_5 for ferric Cyt c and ZnCc. Recent studies indicated that for the overall folding the secondary structure elements of ZnCc and reduced Cyt c are very similar (*38*). In our study, discarding the oxidation state-dependent protein docking difference, we still assume ZnCc is a reliable model of Cyt c in discussing the results.

For the Cyt b_5 E44/48/56A/D60A−Cyt c system, charge neutralization greatly increases the relative contribution of the heme propionate, and some other charged residues surrounding the heme edge (i.e., Glu43, Glu59, Glu37, and Asp66) also contribute to the contact with Cyt c. For the Cyt b_5−DME−Cyt c system, the relative contact frequency of Glu44, Glu48, Glu56, and Asp60 on the surface of Cyt b_5 is similar to that of the Cyt b_5−Cyt c system. However, esterified heme propionate groups do not contribute to the electrostatic interactions. It is consistent with previous studies by Mauk (*39*), which showed that removal of the heme

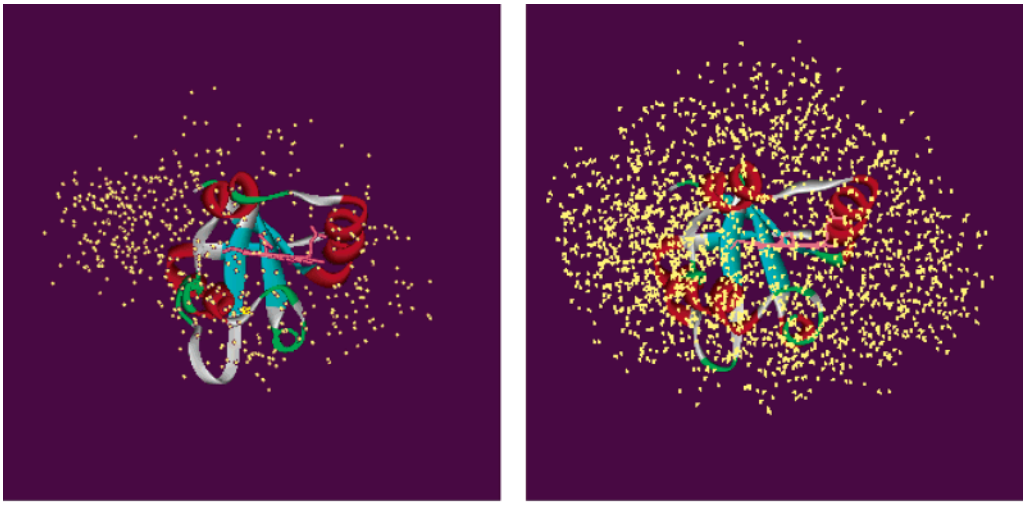

FIGURE 4: Docking profiles for the docking of Cyt b_5 or E44/48/56A/D60A and Cyt *c*. The solid ribbon structures in the middle represent the WT protein and E44/48/56A/D60A Cyt b_5, and the yellow dots represent the centers of mass of the incoming Cyt *c* molecules at the point the distance criterion, a 16 Å C_M-C_M distance in this case, is met. Conditions of the BD simulation are as follows: 100 000 trajectories, ionic strength of 150 mM, and pH 7.0.

propionate substantially reduces the extent of the negative potential and actually shifts its center away from the heme edge. The contact-frequency histograms of the F35Y and V61H mutants of Cyt b_5 are almost the same as that of WT Cyt b_5, considering the residues that are involved in the docking and the relative contribution of those residues. With respect to the Cyt b_5 V45E mutant, the contribution of charged amino acid residues is largely scattered and small compared with that of heme propionate.

DISCUSSION

Docking Geometries that Are Electrostatically and ET Favorable. We initiated these studies with the hypothesis that the elimination of negative charges on the Cyt b_5 surface (i.e., Glu44, Glu48, Glu56, Asp60, and heme propionate) would weaken the formation of the protein complex by weakening the electrostatic attraction of Cyt b_5 for the positively charged Cyt *c*. The UV−visible difference spectroscopic studies confirm this hypothesis. The more charged groups are neutralized, the weaker the binding ability of these two proteins. ET studies by stopped-flow methods and laser-flash photolysis at high ionic strengths also showed that neutralization of these negatively charged residues causes a significant decrease in the ET rate constants, probably reflecting the difficulty of forming a productive ET complex between Cyt b_5 and Cyt *c*. The negatively charged groups of Glu44, Glu48, Glu56, Asp60, and heme propionate do play the most important role in the electrostatically favorable binding geometry.

All the experimental and theoretical facts support the possibility that Glu44, Glu48, Glu56, Asp60, and heme propionate are involved in formation of the electrostatically favorable complex between Cyt b_5 and Cyt *c*. The ET studies at different ionic strengths show that the charge neutralization considerably decreases the ionic strength sensitivity of the ET rates. Thus, the interaction between Cyt b_5 and Cyt *c* must be weakened by surface charge neutralization of Cyt b_5. This is consistent with our BD simulations in that the docking energies are relatively small for those charge-neutralized Cyt b_5 variants. Nevertheless, these surface residues are not the only residues necessary for the ET process, since for the E44/48/56A/D60A−DME Cyt b_5, electron transfer between Cyt b_5 and Cyt *c* can also occur at a relatively fast rate. This is hard to understand if ET only occurs in a unique docking geometry. Undoubtedly, some of the Cyt b_5 mutants must transfer electrons with Cyt *c* in different binding geometries (*12*).

The intraprotein complex ET studies at an ionic strength of 1 mM by laser-flash photolysis showed that esterified heme derivatives decrease the ET rates while neutralization of those surface charged residues, including Glu44, Glu48, Glu56, and Asp60, can increase the ET rates up to 2-fold. Why? Studies on ET in the Cyt *c*−Cyt *c* peroxidase system showed that the orientation that is optimal for binding might not be optimal for electron transfer (*40*, *41*). The potential for more general application of this dynamic docking paradigm is supported by recent studies of the Cyt b_5−myoglobin (Mb) system (*8*, *9*). In the dynamic docking paradigm for protein−protein interactions, numerous weakly bound conformations of the docked complex contribute to the binding of Cyt b_5 to Mb; however, only a very small subset of these are ET active, and this subset need not include the conformations most favorable for binding. Does the Cyt b_5−Cyt *c* system follow this model as well? Can the effects of charge neutralization on ET between Cyt b_5 and Cyt *c* be understood as an enhanced population of the productive ET protein complex?

BD simulations provided insight into the Cyt b_5−Cyt *c* docking. For Cyt b_5 and Cyt *c*, the contact-frequency histograms show that Glu44, Glu48, Glu56, Asp60, and heme propionate of Cyt b_5 are the most important negatively charged groups involved in the docking between these two proteins. When heme propionate is esterified, Glu44, Glu48, Glu56, and Asp60 are still the most important residues in the interactions between Cyt b_5 and Cyt *c*, though the relative populations of these four residues change. It is consistent with Mauk's studies (*39*), which showed that esterification of heme propionate of Cyt b_5 decreases the dipolar magnitude

and shifts the negative center away from the heme-exposed edge. For the Cyt b_5 E44/48/56A/D60A mutant protein, the role of heme propionate is dominant. Other surface charged residues, such as Glu37, Glu43, Glu59, Asp66, etc., replace Glu44, Glu48, Glu56, and Asp60 and help to form the electrostatic protein complexes. However, the relative contributions of these residues are small.

The docking profiles explain things more clearly. On the surface of Cyt b_5, there are many negatively charged groups, including heme propionate, Glu37, Glu38, Glu43, Glu44, Glu48, Glu56, Glu59, Asp60, and Asp66, etc. In the WT Cyt b_5−Cyt c system, Cyt c molecules are located around the heme-exposed edge, especially on the side of Glu44, Glu48, Glu56, and Asp60 in the successfully docked complexes. For the Cyt b_5 E44/48/56A/D60A−Cyt c system, more protein complexes are found, but they are not concentrated. Cyt c actually docks onto a broad surface of Cyt b_5 E44/48/56A/D60A that encompasses essentially the whole hemisphere incorporating the heme edge. Unlike the ET system of the Cyt b_5−Mb complex, charge neutralization does not produce a concentrated ET favorable docking domain. We noticed that the average distance of all the successfully docked complexes between Cyt b_5 E44/48/56A/D60A and Cyt c is ~0.5 Å shorter than that between Cyt b_5 and Cyt c. We assume that the increased intraprotein ET rates possibly result from the decreased donor−acceptor distance between the ET partners.

Our studies of intraprotein complex and interprotein ET support the idea that there must be multiple geometries for docking of Cyt b_5 and Cyt c. The electrostatically favorable docking geometries are not necessarily the same as the ET favorable ones. Charge neutralization of Glu44, Glu48, Glu56, Asp60, and heme propionate weakens the electrostatic interactions, while having actually no essential effect on the intraprotein complex ET. It is more reasonable to conclude that there is a large ensemble of near-optimal ET Cyt b_5−Cyt c complexes. Each possible docking geometry is associated with its own rate constant for ET, which is largely regulated by the conformation and the distance between the reactive centers. As we know, one of the dominant factors for the electron transfer rate is the number of collisions between two protein molecules, which is governed by a number of factors, including temperature, ionic strength, diffusion coefficient, protein concentrations, the driving force of reaction and solvent molecules, etc. However, the effective collision (orientated collision through the ET pathway) essentially contributes to the ET rate. Here, in the Cyt b_5−Cyt c ET system, only the conformations where the two proteins are in nearby "heme edge−heme edge" positions contribute to the ET rate. Since on the heme-containing upper hemisphere of the Cyt b_5 molecule there are more than 10 negatively charged residues, the experimental study and theoretical BD simulation have demonstrated that interaction between Cyt b_5 and Cyt c adapts a dynamic docking mechanism that involves multiple binding orientations for the ET complex formed by the two proteins, facilitating electron transfer through the heme edge. The thermodynamic binding constants measured with UV−visible spectra and NMR are the sum of the individual binding constants for all binding conformations. Each conformation has its own ET rate. For the dynamic docking model, the second-order rate constant, k_2, is the sum of the ET rate constants for all individual conformations, each weighted by the binding constant for individual conformations. It should be noted that Cyt b_5 and Cyt c possess opposite charge with a particular charge distribution on their surface; therefore, the interactions between them are more specific than those between myoglobin and Cyt b_5. As we have concluded above, Cyt b_5−Cyt c binding also occurs with multiple dynamic docking geometries; however, some docking geometries, such as the Salemme model and the Northrup model and the model that we obtained when the E44, E48, E56, and D60 were mutated into alanine (*12*), dominate in the ET.

Contribution of Electrostatic Interactions and Hydrophobic Interactions. Rodgers *et al*. (*3*), via high-pressure techniques coupled with site-directed mutagenesis, reached a conclusion that electrostatics did not provide the main stabilizing factors in the overall association of the Cyt b_5−Cyt c complex. In this report, we present a broad study of the electrostatic interactions (resulting from Glu44, Glu48, Glu56, Asp60, and heme propionate) and hydrophobic interactions (resulting from Val45 and Val61 of Cyt b_5) between Cyt b_5 and Cyt c. Our studies prove that surface charged residues considerably contribute to the strength and specificity of the binding. Studies on Cyt b_5 Val61 mutants do not show a significant effect on the binding constants, as well as the docking geometries obtained from BD simulation. Mutation at Val45 of Cyt b_5 results in some unfavorable changes, shown as small binding constants with Cyt c and scattered docking geometries. Take the V45E mutant as an example; the mutation of Val45 to Glu introduces a large side chain to the interface of the two proteins and leads to unfavorable close contacts between the two cytochrome molecules. To eliminate these close contacts, these two cytochrome molecules have to change their orientations and move away from each other, which would weaken the binding between them. This is consistent with the contact frequency results form BD simulation. These changes probably result from the disturbance of the interface, but not from the loss of the hydrophobic interactions. Therefore, we believe that electrostatic interactions between Cyt b_5 and Cyt c play important roles in the docking alongside hydrophobic interactions.

Is the Surface Hydrophobic Patch of Cyt b_5 a Possible ET Pathway? The UV−visible difference spectroscopic studies show that mutation at Phe35 does not disturb the electrostatic interaction between Cyt b_5 and Cyt c, which is consistent with the contact-frequency histograms obtained from BD simulations. The intraprotein complex ET studies by laser-flash photolysis clearly show that mutation at Phe35 does not perturb the ET rates within the range of error.

As mentioned above, Phe35 as well as Tyr/Phe74 is a component residue of the Cyt b_5 surface hydrophobic patch and of an aromatic channel with His39. Studies on a Tyr74Lys mutant of rat membrane-bound Cyt b_5 demonstrated that Tyr74 is unnecessary for the binding and ET functions of Cyt b_5. Combining the present studies of Phe35 mutants, we conclude that the hydrophobic patch on the surface of Cyt b_5 is not the ET pathway between Cyt b_5 and Cyt c (*42*).

Reorganization Energy. The interprotein ET was studied at an ionic strength of 150 mM by stopped-flow methods

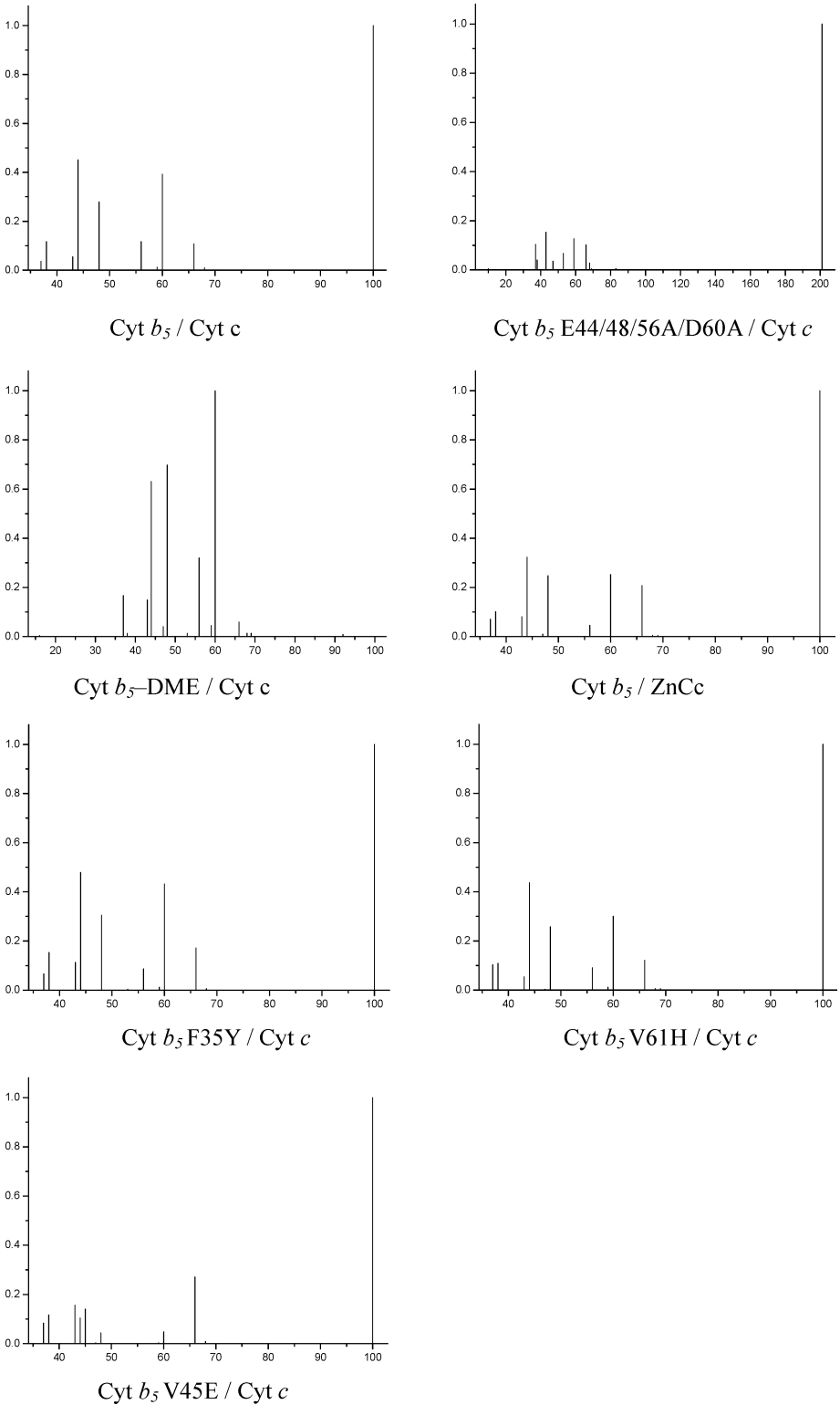

FIGURE 5: Contact histograms of frequencies showing the charged residues of variants of Cyt b_5 involved in ionic contacts with Cyt c residues. The vertical axis frequencies are normalized with the most often contacted residues set as 1. The horizontal axis gives the residue number.

(variants of Cyt b_5 and Cyt c) and laser-flash photolysis (variants of Cyt b_5 and ZnCc).

$$\text{Cyt } b_5\ (Fe^{2+}) + \text{Cyt } c\ (Fe^{3+}) = \text{Cyt } b_5\ (Fe^{3+}) + \text{Cyt } c\ (Fe^{2+})$$

$$\Delta E_0' = 255 \text{ mV}$$

$$^3\text{ZnCc} + \text{Cyt } b_5\ (Fe^{3+}) = {}^{+\bullet}\text{ZnCc} + \text{Cyt } b_5\ (Fe^{2+})$$

$$\Delta E_0' = 875 \text{ mV}$$

As mentioned above, we assume ZnCc is a reliable model of Cyt c in our studies. The primary difference of concern here is the driving force. For the Cyt b_5−Cyt c system, the

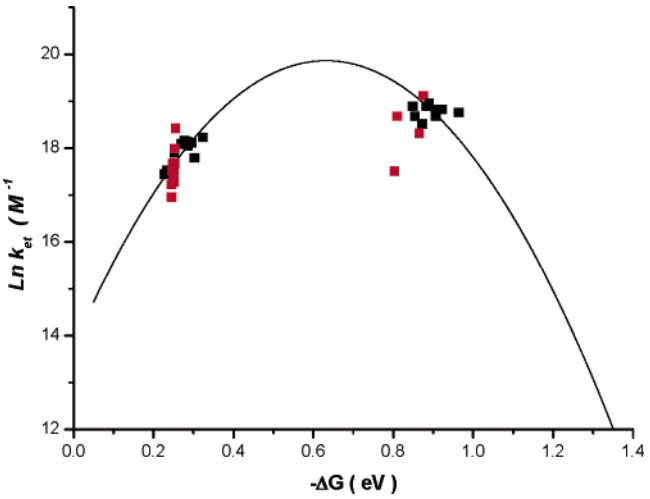

FIGURE 6: Plot of ln k_{et} vs ΔG for the $Fe^{II}b_5$−$Fe^{III}c$ and ^{3}ZnCc−$Fe^{III}b_5$ systems. The solid line is the theoretical fit assuming λ = 0.6 eV and $k = A \exp(-\Delta G + \lambda)^2/(4\lambda kT)$ (classical Marcus theory).

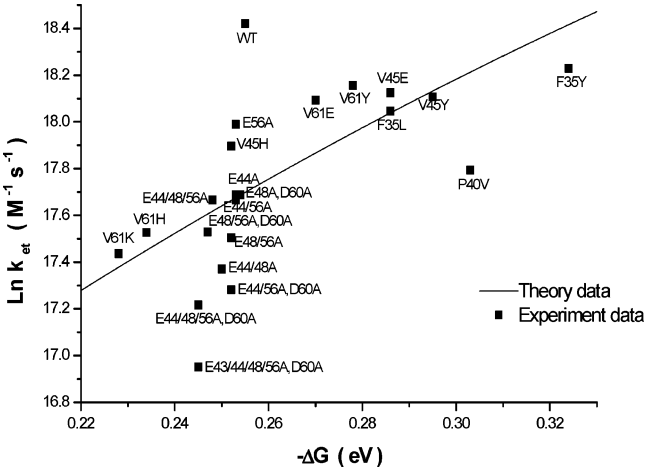

FIGURE 7: Part of Figure 6 (−ΔG varies from 0.22 to 0.34 eV).

driving force is ~255 mV, while for the Cyt b_5−ZnCc system, the driving force is ~875 mV.

Figure 6 displays our ET results and the simulation curve by Marcus theory. The theory curve correlates with our experimental data fairly well. For those Cyt b_5 variants with mutation at the surface charged residues, the ET rates are generally correlated with the binding ability. Meanwhile, for those variants with mutations of hydrophobic residues, the ET rates are roughly correlated with the driving forces, especially in the stopped-flow studies. The ET between Cyt b_5 and ZnCc has a relatively high driving force (~875 mV), so the changes in driving force caused by mutation appear to be screened away under this condition. From the theory curve, we obtain a reorganization energy of 0.6 eV at an ionic strength of 150 mM for the electron transfer between Cyt b_5 and Cyt c, which is comparable with the value of 0.8 eV reported previously (*43*).

CONCLUSIONS

From a series of site-directed mutations on Cyt b_5 and the studies on structure, properties, and reactions with Cyt c, we prefer to describe the ET reaction of the Cyt b_5−Cyt c system as follows. (1) In the Cyt b_5−Cyt c system, electrostatic interaction plays a key role in guiding productive protein docking and generating the orientated collision via the ET pathway. Neutralization of negatively charged residues at the surface alters neither the overall structure nor the redox potential of the proteins; however, the binding affinity between the two proteins is reduced significantly, and the ET rates are decreased as well (shown in Figure 7). Nevertheless, even though Glu44, Glu48, Glu56, Asp60, and the heme propionate, which were nominated by the Salemme model and the Northrup model as key residues in ET, were totally neutralized, the electron transfer between the two proteins does occur. The fact leads to the conclusion that electron transfer in the Cyt b_5−Cyt c system adopts a multiple-docking geometry mechanism, which is also shown by the Brownian dynamic simulation. (2) The redox potential of Cyt b_5 can be regulated by mutation at residues in the heme pocket in the region of −64 to 31 mV. The three-dimensional structure analysis showed that the overall structure is maintained; only local conformational disturbance was observed. Obviously, the mutations did not alter the protein's interface; electron transfer between the two proteins mainly follows the driving force.

ACKNOWLEDGMENT

We are grateful for the kind gifts of the bovine liver microsomal cytochrome b_5 gene from Prof. A. G. Mauk of the University of British Columbia (Vancouver, BC). We thank Associate Prof. Linsen Dai and Mr. Jiuchun Ren for their help with BD simulations and Prof. S. Northrup for supplying the simulation program.

REFERENCES

1. Marcus, R. A., and Sutin, N. (1985) Electron transfers in chemistry and biology, *Biochim. Biophys. Acta 811*, 265−322.
2. McLendon, G. L., and Miller, J. R. (1985) The dependence of biological electron transfer rates on exothermicity: the cytochrome *c*/cytochrome b_5 couple, *J. Am. Chem. Soc. 107*, 7811−7816.
3. Rodgers, K. K., Prochapsky, T. C., and Sligar, S. G. (1988) Probing the mechanisms of macromolecular recognition: the cytochrome b_5-cytochrome *c* complex, *Science 240*, 1657−1659.
4. Burch, A. M., Rigby, S. E. J., Funk, W. D., Macgillivray, R. T. A., Mauk, M. R., Mauk, A. G., and Moore, G. R. (1990) NMR characterization of surface interactions in the cytochrome b_5-cytochrome *c* complex, *Science 247*, 831−833.
5. Mauk, A. G., Mauk, M. R., Moore, G. R., and Northrup, S. H. (1995) Experimental and theoretical analysis of the interaction between cytochrome *c* and cytochrome b_5, *J. Bioenerg. Biomembr. 2*, 311−330.
6. Davydov, D. R. (2001) Microsomal monooxygenase in apoptosis: another target for cytochrome *c* signaling? *Trends Biochem. Sci. 26*, 155−160.
7. Salemme, F. R. (1976) A hypothetical structure for an intermolecular electron transfer complex of cytochrome *c* and cytochrome b_5, *J. Mol. Biol. 239*, 1018−1023.
8. Northrup, S. H., Thomasson, K. A., and Miller, C. M. (1993) Effect of charged amino acid mutatuons on the bimolecular kinetics of reduction of yeast iso-1-ferricytochrome *c* by bovine ferrocytochrome b_5, *Biochemistry 32*, 6613−6623.
9. Guillemette, J. G., Barker, P. D., Eltis, L. D., Smith, T. P., Lo, M., Brayer, G. D., and Mauk, A. G. (1994) Analysis of the bimolecular reduction of ferricytochrome *c* by ferrocytochrome b_5 through mutagenesis and molecular modelling, *Biochimie 76*, 592−604.
10. Qian, C. M., Yao, Y., Ye, K. Q., Wang, J. F., Tang, W. X., Wang, Y. H., Wang, W. H., Lu, J. X., Xie, Y., and Huang, Z. X. (2001) Effects of charged amino-acid mutation on the solution structure of cytochrome b_5 and binding between cytochrome b_5 and cytochrome *c*, *Protein Sci. 10*, 2451−2459.
11. Wu, Y. B., Wang, Y. H., Qian, C. M., Lu, J., Li, E. C., Wang, W. H., Lu, J. X., Xie, Y., Wang, J. F., Zhu, D. X., Huang, Z. X., and

Tang, W. X. (2001) Solution structure of cytochrome b_5 mutant (E44/48/56A/D60A) and its interaction with cytochrome *c*, *Eur. J. Biochem. 268*, 1620−1630.
12. Wu, J., Gan, J.-H., Wang, Y.-H., Wang, W.-H., Sun, B.-Y., Huang, Z.-X., and Xia, Z.-X. (2002) Molecular recognition and interprotein binding of cytochrome b_5 with cytochrome *c*, *Chin. J. Chem. 20* (11), 1225−1234.
13. Liang, Z. X., Jiang, M., Ning, Q., and Hoffman, B. M. (2002) Dynamic docking and electron transfer between myoglobin and cytochrome b_5, *J. Biol. Inorg. Chem. 7*, 580−588.
14. Liang, Z. X., Nocek, J. M., Huang, K., Hayes, R. T., Kurnikov, I. V., Beratan, D. N., and Hoffman, B. M. (2002) Dynamic docking and electron transfer between Zn-myoglobin and cytochrome b_5, *J. Am. Chem. Soc. 124*, 6849−6859.
15. Sun, Y. L., Wang, Y. H., Yan, M. M., Sun, B. Y., Xie, Y., Huang, Z. X., Jiang, S. K., and Wu, H. M. (1999) Structure, interaction and electron transfer between cytochrome b_5, its E44A and/or E56A mutants and cytochrome *c*, *J. Mol. Biol. 285*, 347−359.
16. Gan, J. H., Wu, J., Wang, Z. Q., Wang, Y. H., Huang, Z. X., and Xia, Z. X. (2002) Structures of V45E and V45Y mutants and structure comparison of a variety of cytochrome b_5 mutants, *Acta Crystallogr. D58*, 1298−1306.
17. Wu, J., Gan, J. H., Xia, Z. X., Wang, Y. H., Wang, W. H., Xue, L. L., Xie, Y., and Huang, Z. X. (2000) Crystal structure of recombinant trypsin-solubilized fragment of cytochrome b_5 and the structural comparison with Val61His mutant, *Proteins: Struct., Funct., Genet. 40*, 249−257.
18. Wang, Y. H., Wang, W. H., Lu, J. X., Ren, Y., Gu, S. H., Xie, Y., and Huang, Z. X. (2001) Preparation and characterization of some surface negatively charged residue mutants of cytochrome b_5, *Chin. Sci. Bull. 46*, 555−558.
19. Wang, Y. H., Ren, Y., Wang, W. H., Xie, Y., and Huang, Z. X. (2001) The regulation of surface charged residues on the properties of cytochrome b_5, *J. Protein Chem. 20*, 487−493.
20. Yao, P., Xie, Y., Wang, Y.-H., Sun, Y.-L., Huang, Z.-X., Xiao, G.-T., and Wang, S.-D. (1997) Importance of a conserved phenylalanine35 of cytochrome b_5 to its stability and redox potential, *Protein Eng. 10*, 575−581.
21. Wang, Z.-Q., Wang, Y.-H., Qian, W., Wang, H.-H., Chunyu, L.-J., Xie, Y., and Huang, Z.-X. (1998) Methanol-induced unfolding and refolding of cytochrome b_5 and its P40V mutant monitored by UV−visible, CD, and fluorescence spectra, *J. Protein Chem. 18*, 547−555.
22. Wang, Y. H., Lu, J. X., Wang, W. H., Ren, Y., Xie, Y., and Huang, Z. X. (2002) Role of Phe58 residue in stabilizing structure of cytochrome b_5, *Chin. Sci. Bull. 47*, 2063−2066.
23. Wang, Z. Q., Wang, W. H., Wang, W. H., Xue, L. L., Wu, X. Z., Xie, Y., and Huang, Z. X. (2000) The effect of mutation at valine-45 on the stability and redox potentials of trypsin-cleaved cytochrome b_5, *Biophys. Chem. 83*, 3−17.
24. Xue, L. L., Wang, Y. H., Xie, Y., Yao, P., Wang, W. H., Qian, W., and Huang, Z. X. (1999) Effect of Mutation at Valine 61 on the Three-Dimensional Structure, Stability, and Redox Potential of Cytochrome b_5, *Biochemistry 38*, 11961−11972.
25. Reid, L. S., Mauk, M. R., and Mauk, A. G. (1984) Role of heme propionate groups in cytochrome b_5 electron transfer, *J. Am. Chem. Soc. 106*, 2182−2185.
26. Vanderkooi, J. M., Adar, F., and Erecinska, M. (1976) Metallocytochromes *c*: characterization of electronic absorption and emission spectra of Sn^{4+} and Zn^{2+} cytochromes c, *Eur. J. Biochem. 64*, 381−387.
27. Vanderkooi, J. M., and Erecinska, M. (1976) Cytochrome *c* interaction with membranes: Absorption and emission spectra and binding characterizaiton of iron-free cytochrome *c*, *Eur. J. Biochem. 60*, 199−207.
28. Ye, S., Shen, C., Cotton, T. M., and Kostic, N. M. (1997) Characterization of zinc-substituted cytochrome *c* by circular dichroism and resonance Raman spectroscopy methods, *J. Inorg. Biochem. 65*, 219−226.
29. Moffet, D. A., Case, M. A., House, J. C., Vogel, K., Williams, R. D., Spiro, T. G., McLendon, G. L., and Hecht, M. H. (2001) Carbon monoxide binding by *de novo* heme proteins derived from designed combinatorial libraries, *J. Am. Chem. Soc. 123* (10), 2109−2115.
30. Goldbeck, R. A., and Kliger, D. S. (1993) Nanosecond time-resolved absorption and polarization dichroism spectroscopies, *Methods Enzymol. 226*, 147−177.
31. Hofrichter, J., Ansari, A., Jones, C. M., Deutsch, R. M., Sommer, J. H., and Henry, E. R. (1994) Ligand binding and conformational changes measured by time-resolved absorption spectroscopy, *Methods Enzymol. 232*, 387−415.
32. Northrup, S. H., Boles, J. O., and Reynolds, J. C. L. (1988) Brownian dynamics of cytochrome *c* and cytochrome *c* peroxidase association, *Science 241*, 67−70.
33. Northrup, S. H., Thomasson, K. A., Miller, C. M., Barker, P. D., Eltis, L. D., Guillemette, J. G., Inglis, S. C., and Mauk, A. G. (1993) Effects of charged amino acid mutations on the bimolecular kinetics of reduction of yeast iso-1-ferricytochrome *c* by bovine ferrocytochrome b_5, *Biochemistry 32*, 6613−6623.
34. Mauk, M. R., Reid, L. S., and Mauk, A. G. (1982) Spectrophotometric analysis of the interaction between cytochrome b_5 and cytochrome *c*, *Biochemistry 21*, 1843−1846.
35. Wang, Z. Q., Wu, J., Wang, Y. H., Qian, W., Xie, Y., Xia, Z. X., and Huang, Z. X. (2002) Effect of Mutation at Proline-40 of Cytochrome b_5 on the Protein Structure, Stability and Functions, *Chin. J. Chem. 20* (11), 1212−1224.
36. Qin, L., and Kostic, N. M. (1994) Photoinduced electron transfer from the triplet state of zinc cytochrome *c* to ferricytochrome b_5 is gated by configurational fluctuations of the diprotein complex, *Biochemistry 33* (42), 12592−12599.
37. Furukawa, Y., Ishimori, K., and Morishima, I. (2002) Oxidation-state-dependent protein docking between cytochrome *c* and cytochrome b_5: high-pressure laser flash photolysis study, *Biochemistry 41*, 9824−9832.
38. Qian, C. M., Yao, Y., Tong, Y. F., Wang, J. F., and Tang, W. X. (2003) Structural analysis of zinc-substituted cytochrome *c*, *J. Biol. Inorg. Chem. 8*, 394−400.
39. Mauk, M. R., and Mauk, A. G. (1986) Electrostatic analysis of the interaction of cytochrome *c* with native and dimethyl ester heme substituted cytochrome b_5, *Biochemistry 25*, 7085−7091.
40. Erman, J. E., Kresheck, G. C., Vitello, L. B., and Miller, M. A. (1997) Cytochrome *c*/cytochrome *c* peroxidase complex: effect of binding-site mutations on the thermodynamics of complex formation, *Biochemistry 36*, 4054−4060.
41. Cheung, E., Taylor, K., Kornblatt, J. A., English, A. M., McLendon, G., and Miller, J. R. (1986) Direct measurements of intramolecular electron transfer rates between cytochrome *c* and cytochrome *c* peroxidase: effects of exothermicity and primary sequence on rate, *Proc. Natl. Acad. Sci. U.S.A. 83*, 1330−1333.
42. Yao, P., Wang, Y.-H., Sun, B.-Y., Xie, Y., Hirota, S., Yamauchi, O., and Huang, Z.-X. (2002) Kinetic studies on the oxidation of cytochrome b_5 Phe35 mutants with cytochrome *c*, plastocyanin and complexes, *J. Biol. Inorg. Chem. 7*, 375−383.
43. McLendon, G., and Hake, R. (1992) Interprotein electron transfer, *Chem. Rev. 92*, 481−490.

BI036078K